Revista Brasileira de Meteorologia, **v. 37, n. 1,** 99−119, 2022 rbmet.org.br
DOI: http://dx.doi.org/10.1590/0102-7786370075

Artigo

Assessment of Climate Change Using Humidity index of Thornthwaite Climate Classification in Pantanal Biome

João Antonio Lorençone[1], Lucas Eduardo de Oliveira Aparecido[2],
Pedro Antonio Lorençone[1], Rafael Fausto de Lima[1], Guilherme Botega Torsoni[3]

[1]Departamento de Agrometereologia, Instituto Federal de Mato Grosso do Sul, Naviraí, MS, Brazil.
[2]Departamento de Agrometereologia, Instituto Federal do Sul de Minas, Muzambinho, MG, Brazil.
[3]Departamento de Agrometereologia, Instituto Federal do Sul de Minas, Muzambinho, MG, Brazil.

Received: 13 January 2021 - Accepted: 5 February 2022

Abstract

Thornthwaite climate classification indices are essential to interpret climate types in the state of the pantanal biome (Mato Grosso do Sul), simplifying calculation process and interpretation of climatological water balance by farmers. However, there are few studies found in the literature that characterize the climate of pantanel biome in different climatic scenarios. We seek to assess climate change using humidity index of Thornthwaite climate classification in pantanal biome. We used historical series of climate data from all 79 municipalities of Mato Grosso do Sul between 1987 and 2017, which were divided into microregions. Air temperature and precipitation were collected on a daily scale. Precipitation and potential evapotranspiration data allowed calculating water balance by the Thornthwaite and Mather method. We characterized all locations as wet and dry using aridity indices proposed by Thornthwaite. The global climate model used was BCC-CSM 1.1 developed at the Beijing Climate Center (BCC) with a resolution of 125 x 125 km. We used the scenarios RCP-2.6, RCP-4, RCP-6 and RCP-8.5 for analyzing 21st century projections (2041-2060 and 2061-2080 periods). Maps were generated from climate indices of Mato Grosso do Sul using kriging interpolation method with spherical model, one neighbor, and 0.25° resolution. The microregions showed different patterns regarding water balance components and humidity index. Humidity index had a mean of 15.94. The prevailing climate in the state of Mato Grosso do Sul is C2 (moist subhumid). The state of Mato Grosso do Sul has two well-defined periods during the year: a dry and a rainy period. Three climate types predominate in Mato Grosso do Sul and, according to the Thornthwaite classification, are B1 (humid), C2 (moist subhumid), and C1 (dry subhumid). Water characterization in Mato Grosso do Sul showed 234.78 mm year^{-1} of water surplus, 80.8 mm year^{-1} of water deficit, and 1,114.8 mm year^{-1} of potential evapotranspiration. Water deficit and potential evapotranspiration decrease as latitude increases. The climatic projections show, in all scenarios, reduce the area classified as umida in the state (B1, B2 and B3), besides adding the dry subhumid class (C1). The Scenario RCP 8.5 in 2061 - 2080 is the most worrisome situation of all, because the state can undergo major changes, especially in the pantanal biome region.

Keywords: IPCC, climatology, water deficit, humid zoning, Brazil.

Avaliação das Mudanças Climáticas Usando o Índice de Humidade da Classificação Climática Thornthwaite no Bioma Pantanal

Resumo

Os índices de classificação climática Thornthwaite são essenciais para interpretar os tipos de clima no estado do bioma pantanal (Mato Grosso do Sul), simplificando o processo de cálculo e interpretação do equilíbrio climatológico da água pelos agricultores. Contudo, existem poucos estudos encontrados na literatura que caracterizam o clima do bioma pantaneiro em diferentes cenários climáticos. Procuramos avaliar as alterações climáticas utilizando o índice de humidade da classificação climática de Thornthwaite no bioma pantaneiro. Utilizámos séries históricas de dados climáticos de todos os 79 municípios de Mato Grosso do Sul entre 1987 e 2017, que foram divididos em microrregiões. A temperatura

Autor de correspondência: Lucas Eduardo de Oliveira Aparecido, lucas.aparecido@ifsuldeminas.edu.br

do ar e a precipitação foram recolhidas numa escala diária. Os dados de precipitação e evapotranspiração potencial permitiram calcular o balanço hídrico pelo método de Thornthwaite e Mather. Caracterizámos todos os locais como húmidos e secos utilizando índices de aridez propostos por Thornthwaite. O modelo climático global utilizado foi BCC-CSM 1.1 desenvolvido no Centro Climático de Pequim (BCC) com uma resolução de 125 x 125 km. Utilizámos os cenários RCP-2.6, RCP-4, RCP-6 e RCP-8.5 para analisar projecções do século XXI (períodos 2041-2060 e 2061-2080). Foram gerados mapas a partir de índices climáticos de Mato Grosso do Sul usando o método de interpolação kriging com modelo esférico, um vizinho, e resolução de 0,25°. As microrregiões mostraram diferentes padrões no que diz respeito aos componentes do balanço hídrico e índice de humidade. O índice de humidade tinha uma média de 15,94. O clima predominante no estado de Mato Grosso do Sul é C2 (sub-húmido húmido). O estado de Mato Grosso do Sul tem dois períodos bem definidos durante o ano: um período seco e um período chuvoso. Três tipos de clima predominam em Mato Grosso do Sul e, de acordo com a classificação Thornthwaite (1948), são B1 (húmido), C2 (sub-húmido húmido), e C1 (sub-húmido seco). A caracterização da água em Mato Grosso do Sul mostrou 234,78 mm ano^{-1} de excesso de água, 80,8 mm ano^{-1} de défice hídrico, e 1.114,8 mm ano^{-1} de evapotranspiração potencial. O défice de água e a evapotranspiração potencial diminuem à medida que a latitude aumenta. As projecções climáticas mostram, em todos os cenários, reduzir a área classificada como umida no estado (B1, B2 e B3), além de adicionar a classe seca sub-húmida (C1). O Cenário RCP 8.5 em 2061 - 2080 é a situação mais preocupante de todas, porque o estado pode sofrer grandes alterações, especialmente na região do bioma pantanal.

Palavras-chave: IPCC, climatologia, déficit hídrico, zoneamento húmido, Brasil.

1. Introduction

Climatic characterization is indispensable to define and analyze regional climates, mainly for agricultural development (Ceglar *et al*., 2016; Sissoko *et al*., 2011). The climate can be considered as the average of atmospheric conditions for 30 years (Passos *et al*., 2016). (Aparecido *et al*., 2016) highlight that climate can be defined by climate classification systems, which are methods to determine the climate classes of a given region. Agriculture is an economic activity greatly affected by weather conditions (de Sá Júnior *et al*., 2012), as weather elements vary both geographically and seasonally, and can promote high damage to crops.

The water available in the soil is a determining factor in the development of plants, being essential to complete the phenological cycle, impacting the final productivity of crops (Abrecht and Carberry, 1993; Akas *et al*., 2019). The climatological water balance (CWB) makes it possible to quantify the water available in the soil in a given period, helping to monitor the development of plants and thus agricultural planning (Brunel-Saldias *et al*., 2018; Mohammad et al., 2018, Cecílio *et al*., 2012) reported that the CWB is sensitive to various climatic conditions, especially air temperature and precipitation, and it is important to carry out a seasonal and regional assessment.

There are several methods of estimating CWB in the international literature, but the methodology of (Thornthwaite and Mather, 1955) is the most used, as it presents a simplified and practical way to obtain soil water storage. CWB output variables allow the climate classification of several areas (Dantas *et al*., 2007). (Thornthwaite, 1948) climate classification system is considered the most important in studies of agriculture, ecology, and water resources, precisely because it uses CWB in its methodology. In this classification, the plant is considered the physical medium by which it is possible to carry water from soil to the atmosphere (Rolim *et al*., 2007). In addition, Thornthwaite (1948) climate classification is based on humidity indices (Feddema, 2005) and thermal efficiency (Elguindi *et al*., 2014), and has CWB as a reference (Passos *et al*., 2016).

In recent years climate change has become a major problem for humanity (Holm and Winiwarter, 2017). In the last century, the global temperature has increased by 1 °C (+−0.2), forecasts for 2100 are for increases between 1.5 °C and 6 °C (Adefisan, 2018; IPCC, 2014). Changes in the current climate can alter the entire water classification of a region, impacting ecosystems and thus economic activities (Thayer *et al*., 2020). Thus, studies on the impact of climate projections on the water behavior of the regions are fundamental to minimize the damage to various economic activities, such as agriculture (Michalak, 2020).

We seek to assess climate change using humidity index of Thornthwaite climate classification in pantanal biome.

2. Materiais e Métodos

The study was carried out in the state of Mato Grosso do Sul (MS), main region with pantanal biome in Brazil. The state has an area of 357,145.32 km^2, with 79 municipalities. Altitudes of MS range from 24 to 1000 m. This state has stood out in the agricultural area since the fourth year of its creation, surpassing the national average in harvested area. Agribusiness is the predominant activity in the state due to the richness of soils and favorable climate conditions (Casonato, 2013).

The climate data used were collected for all 79 municipalities of Mato Grosso do Sul, between 1987 and 2017, maximum period of data available on the platform, which were divided into microregions (Fig. 1). Air temperature (T_{air}, °C) and precipitation (P, mm) were collected on a daily scale from NASA/POWER platform.

The collected data were used to estimate potential evapotranspiration (ETP) using the Camargo (1971) method (Eq. (1)), because it is designed for the region of the state of São Paulo, and demonstrates high efficiency using only the air temperature as input (Aparecido *et al.*, 2020; Cunha *et al.*, 2017; Pereira and Paes De Camargo, 1989). The criterion for choosing this model was the data availability.

$$ETP = 0.01 \times \left(\frac{Qo}{2.45}\right) \times T_{air} \times ND \tag{1}$$

where Qo is the solar irradiance at the top of the atmosphere (MJ m^{-2} day^{-1}), Tair is the mean air temperature (°C), and ND is the number of days.

The water balance (WB) proposed by Thornthwaite and Mather (1955) was calculated with an available water capacity in the soil (AWC) equal to 100 mm, which represents a large part of agricultural crops, in addition to being the most used value in studies for soil moisture (Mhlanga and Thierfelder, 2021; Pagliai *et al.*, 2004). Soil water storage (SWS), water deficit (DEF), and water surplus (EXC) of the soil-plant-atmosphere system were estimated according to Eqs (2) to (7):

$$If\ (P-ETP)_i < 0 = \begin{cases} NAC_i = NAC_{i-1} + (P-ETP)_i \\ SWS = AWC\, e^{\frac{(NAC)_i}{AWC}} \end{cases} \tag{2}$$

$$If\ (P-ETP)_i \geq 0 = \begin{cases} NAC_i = AWC\ ln\dfrac{SWS_i}{AWC} \\ SWS = (P-ETP)_i + SWS_{i-1} \end{cases} \tag{3}$$

$$ALT_i = SWS_i - SWS_{i-1} \tag{4}$$

$$ETR_i = \begin{cases} P + |ALT_i|, & if\ ALT < 0 \\ ETP_i, & if\ ALT \geq 0 \end{cases} \tag{5}$$

$$DEF = ETP - ETR \tag{6}$$

$$EXC_i = \begin{cases} 0, & if\ AWC < 0 \\ (P-ETP)_i - ALT_i & if\ AWC = 0 \end{cases} \tag{7}$$

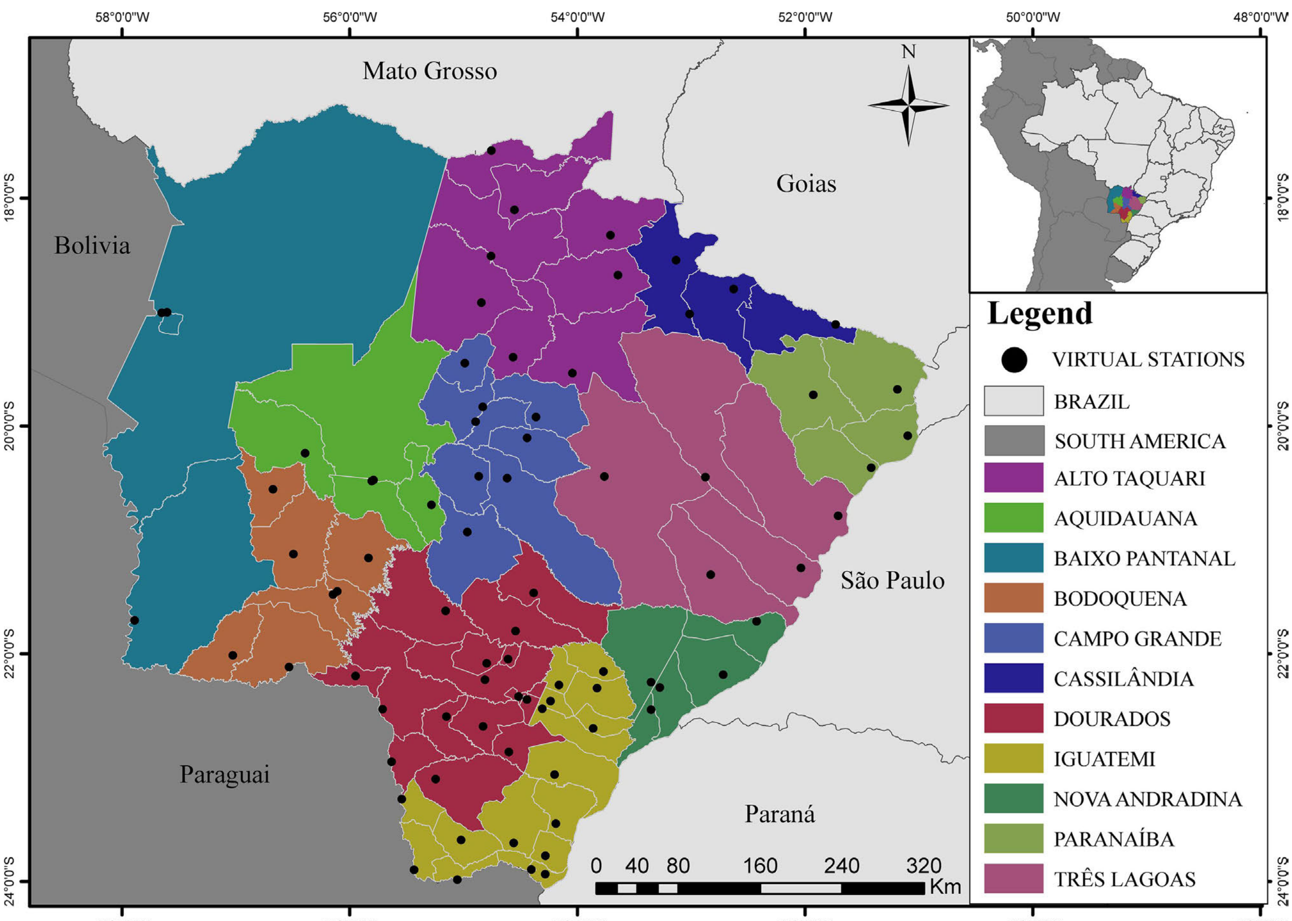

Figure 1 - Location of the microregions of the state of Mato Grosso do Sul and the virtual stations studied.

where *ETP* is the potential evapotranspiration (mm), *AWC* is the available water capacity in the soil (mm), *SWS* is the soil water storage (mm), *NAC* is the accumulated negative, i.e., accumulated precipitation minus potential evapotranspiration, *P* is the precipitation (mm), *DEF* is the water deficit in the soil-plant-atmosphere system (mm), ETR is the real evapotranspiration (mm), *EXC* is the water surplus of the soil-plant-atmosphere system (mm), *ALT* is the soil water storage for the current month minus soil water storage for the previous month (mm), and i is the monthly period.

Box-plots with the mean, median, and outlier points were prepared for the distribution and variation in weather elements. These analyses are essential to understand the climate within each microregion in the state of MS and enable the comparison between regions.

The aridity indices proposed by Thornthwaite (1948) were used to characterize the studied locations as wet and dry. The calculations of aridity, water, and humidity indices were processed according to Eqs (9) to (11).

$$I_w = \frac{EXC}{ETP} \times 100 \tag{9}$$

$$I_a = \frac{DEF}{ETP} \times 100 \tag{10}$$

$$I_h = I_h - 0.6 \times I_a \tag{11}$$

where *Iw* is the water index, *Ia* is the aridity index, *Ih* is the humidity index, *EXC* and *DEF* are the water surplus and deficit (mm), respectively, both from the climatological water balance, and *ETP* is the reference or potential evapotranspiration (mm).

Thornthwaite and Mather climate classification key based on the humidity index: $100.0 \leq Ih$ is A - Perhumid; $80.0 \leq Ih < 100.0$ is B4 - Humid; $60.0 \leq Ih < 80.0$ is B3 - Humid; $40.0 \leq Ih < 60.0$ is B2 - Humid; $20.0 \leq Ih < 40.0$ is B1 - Humid; $00.0 \leq Ih < 20.0$ is C2 - Moist subhumid; $-33.3 \leq Ih \geq 00.0$ is C1 - Dry subhumid; $-66.7 \leq Ih < -33.3$ is D - Semiarid and $-100 \leq Ih < -66.7$ is E - Arid (Ometto, 1981).

The climate indices calculated for MS allowed generating maps using the kriging interpolation method (Krige, 1951), with the spherical model, one neighbor, and a 0.25° (25 km) resolution.

The data from the IPCC are the result of simulations of global models of some research centers that contribute to the preparation of the IPCC-AR5 report, forced by the observed concentrations of greenhouse gases during the twentieth century and forced by an estimated concentration for the 21st century (Boer *et al*., 2000). The global climate model used was the BCC - CSM 1.1 developed at the Beijing Climate Center (BCC), has a resolution of 125 × 125 km, with 26 vertical levels, its components are: atmosphere, earth surface, ocean, sea ice, terrestrial carbon cycle, biogeochemical cycles of the ocean (Flato *et al*., 2014).

Representative Concentration Pathways (RCPs), serve as input for climate modeling and atmospheric chemistry in cmip5 numerical experiments, they receive their names from the levels of the radioactive forces, in W.m^{-2} (Hartin *et al*., 2015). In this work, rcp2.6, RCP4., RCP6 scenarios will be used. and RCP8.5 for analysis of 21st century projections. All steps to carry out the work are represented in the flowchart (Fig. 2).

3. Resultados e Discussão

Air temperature in the state of Mato Grosso do Sul presented a pattern in the monthly variation for microregions (Fig. 3A). Monthly air temperature values of microregions ranged from 17 to 29 °C, with a mean annual air temperature of 24 °C. The high air temperatures in the state occurred from January to April and November to December, with a mean of 26 °C. However, air temperature decreased from May to July, with a mean of 20 °C. The microregions of Baixo Pantanal (west) and Iguatemi (south) stood out among the localities with the highest and lowest air temperatures, respectively, with annual means of 27 and 23 °C.

The accumulated mean annual precipitation of Mato Grosso do Sul was 1,379 mm (Fig. 3B). Precipitation concentration and distribution in the state were uneven. The lowest precipitation values were observed from June to September. However, precipitations increased from January to May and October to December. Iguatemi microregion, located in the south of the state, showed the highest annual precipitation, with a value of 1,472 mm. These variations in air temperature and precipitation over the year may affect the development and productivity of crops in the state of Mato Grosso do Sul because, among economic activities, agriculture is the most vulnerable to climate variability (Geng *et al*., 2016; Hossain *et al*., 2002).

Microregions showed different patterns in the water balance components and humidity index, as shown in Fig. 4. The annual potential evapotranspiration (ETP) of Mato Grosso do Sul was 1,116.52 mm (± 62.21 mm), as shown in Fig. 4A. Baixo Pantanal and Aquidauana microregions, both located in the west of the state, had the highest annual ETP values.

Nova Andradina and Três Lagoas, located in the east of MS, had values above 1000 mm, which is below the mean of the annual ETP in the state. Alto Taquari, in the north, presented the highest ETP variation. Microregions located in the northwest presented the highest potential evapotranspiration, as their increase is related to an

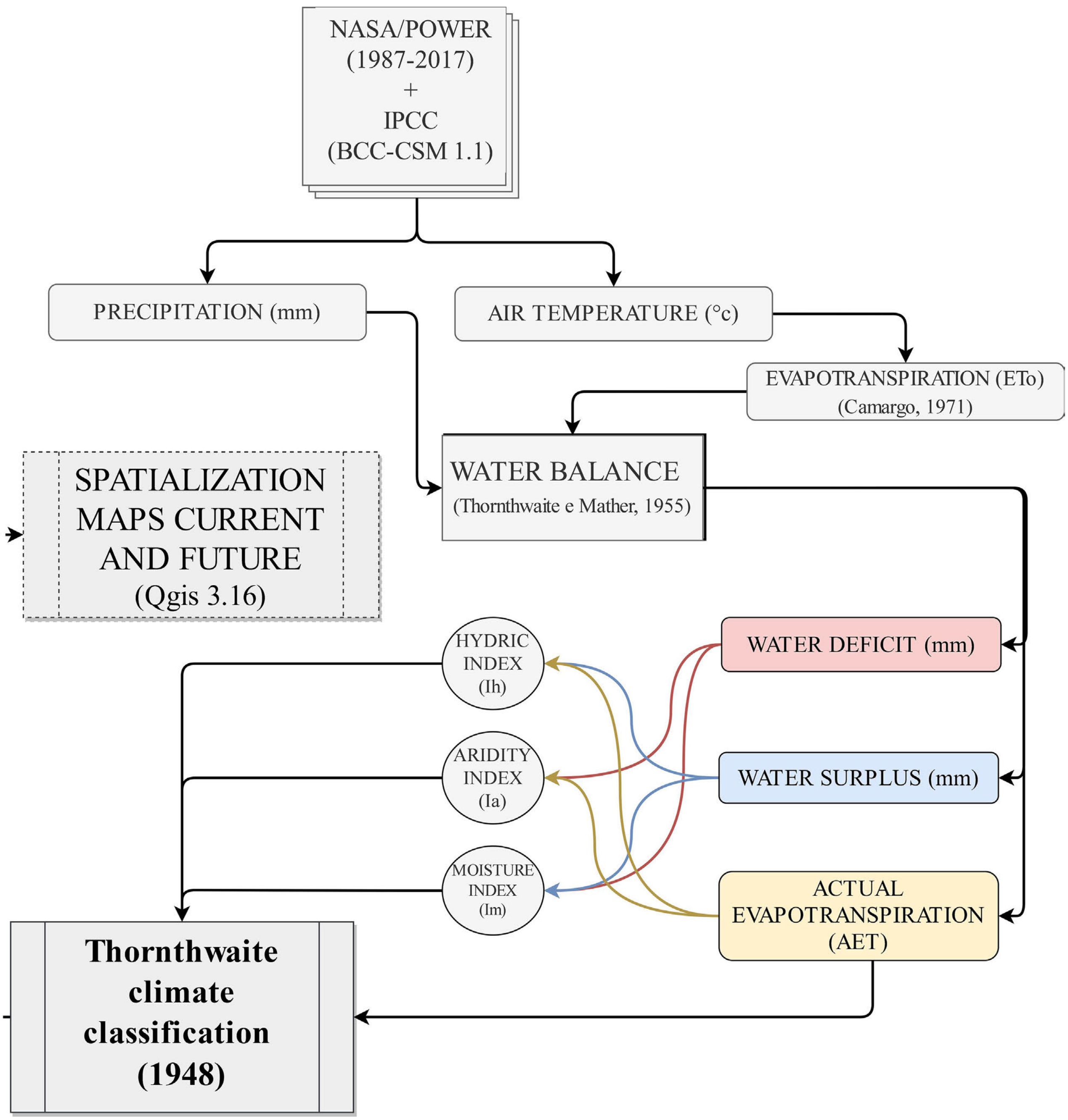

Figure 2 - Flowchart describing the steps to carry out the work

increase in the radiation balance, advective effect, air temperature, and decrease in relative humidity.

The water surplus (EXC) of MS showed a mean annual value of 234.8 mm (± 121.04 mm), as shown in Fig. 4B. Iguatemi and Dourados had the highest variations in water surplus. Microregions of Cassilândia and Alto Taquari, both located in the north, and Parnaíba (east) showed a normal distribution of water surplus results. The pattern of inter-annual EXC distribution in the microregions was similar.

Aquidauana, Baixo Pantanal, and Bodoquena presented water surplus below the mean annual value for MS. Among microregions, Cassilândia had the highest mean annual water surplus, with a value of 429.17 mm (± 41.1 mm), this region concentrates two rivers that raise air and soil humidity in the region, providing warmer winters, in addition to more frequent rains in the summer period (Zortéa *et al.*, 2021). Baixo Pantanal had the lowest water surplus, with a value of 23.15 mm (± 23.61 mm). The muni-

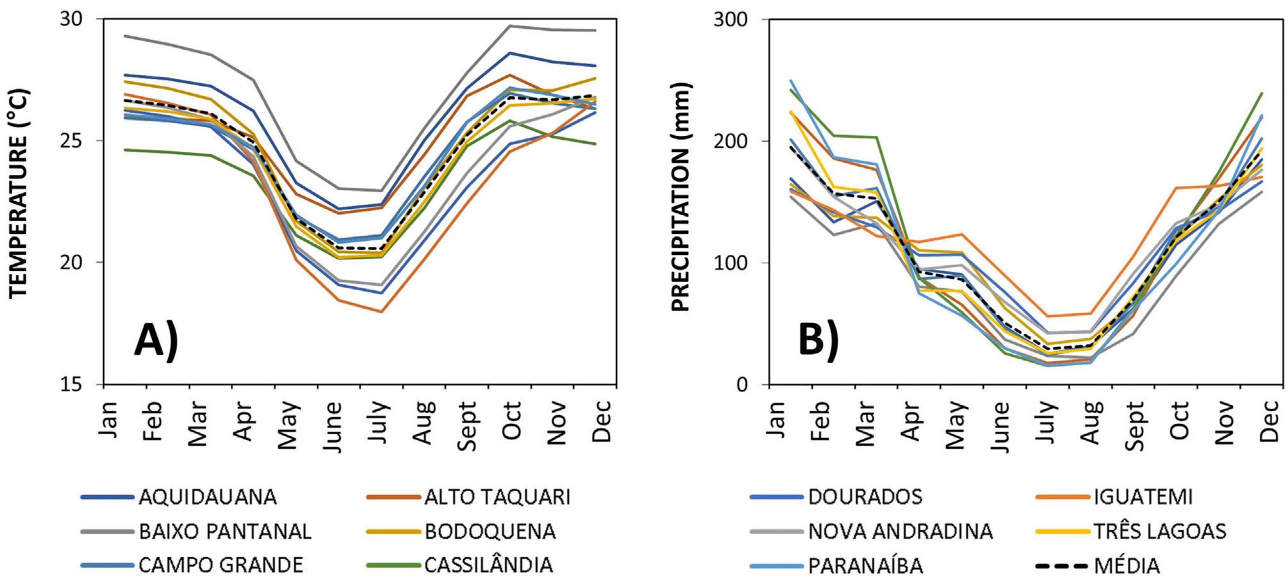

Figure 3 - Monthly variation (A) of air temperature (°C) and (B) precipitation (mm) for microregions of the state of Mato Grosso do Sul (MS).

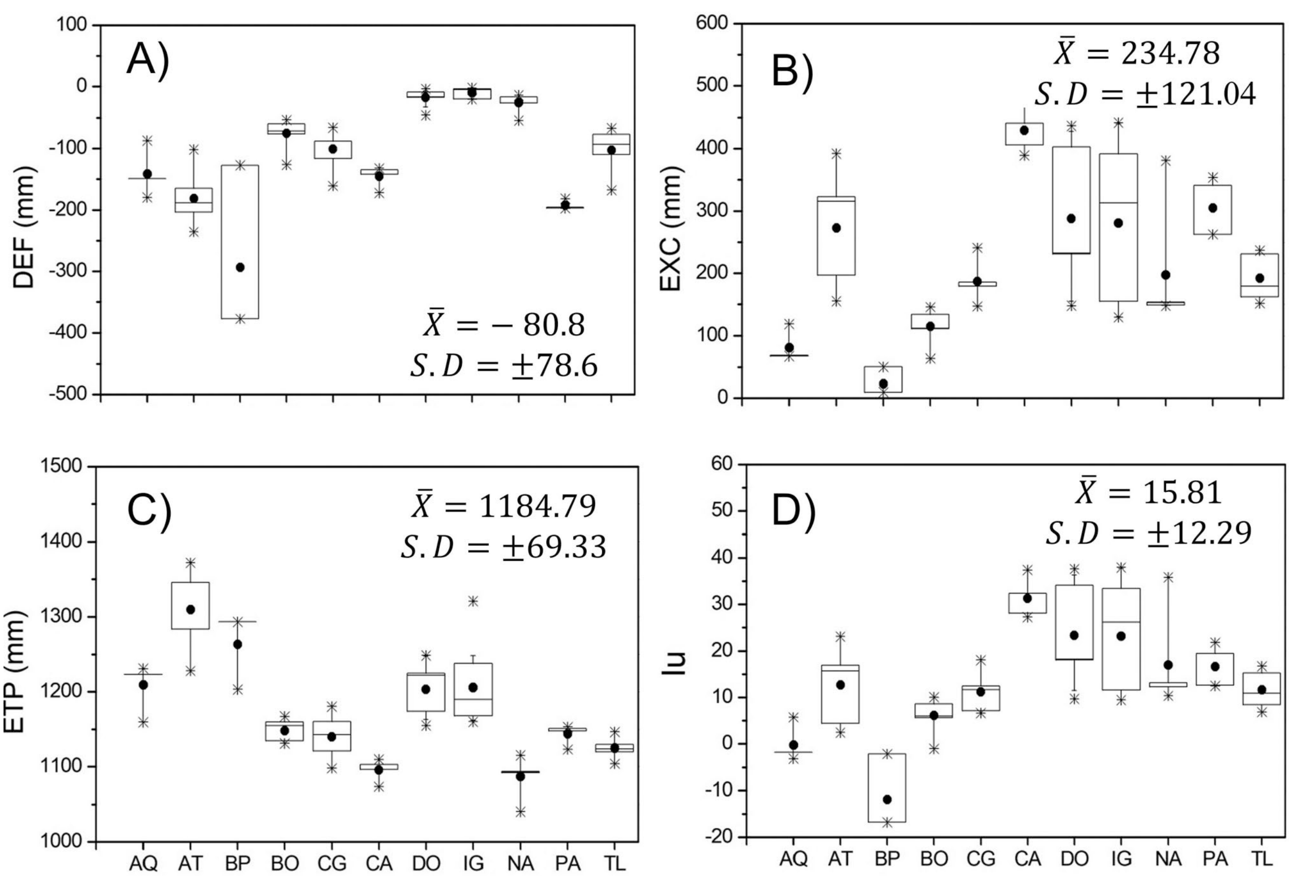

Figure 4 - Box plot graphs of potential evapotranspiration (A), water deficit (B), water surplus (C), and humidity index for microregions of the state of Mato Grosso do Sul.

cipalities Chapadão do Sul, Sete Quedas, and Costa Rica presented the highest EXC values, all above 440 mm per year.

However, Baixo Pantanal had the highest water deficit and variation in results (Fig. 3A). Ladário and Corumbá, two municipalities in the region, presented the highest DEF values in the state. In the Pantanal region, drought is common for most of the year, due to high temperatures and reduced rainfall, drying up the rivers in the region. (Clarke, 2005; Lopes Ribeiro et al., 2021). Supplementary irrigation can be a strategy for the stability and productivity of crops in the driest microregions of the state, as its use during drought periods minimizes productivity losses (Montoya *et al*., 2017).

The humidity index (Ih) presented a mean of 15.94 (± 11.57), as shown in Fig. 4D. Baixo Pantanal showed the lowest Ih, with a value of −11.89 (± 8.43), and Cassilândia microregion had the highest Ih, with a value of 31.26 (± 4.65), showing a relationship with DEF and EXC in the microregions. The results of Ih from Cassilândia and Paranaíba showed a normal distribution, i.e., it showed no much variation. Iguatemi and Dourados, on the other hand, showed the highest variation.

The mean annual water surplus in MS was 234.8 mm (± 134.2 mm). A water surplus was observed from January to July and September to December in the state. The highest water surplus was observed in January, with a value of 52.7 mm. The water deficit in MS was 84.06 mm (± 87.28 mm). The highest water deficit in MS was observed from May to November. August was the driest month in the state, with 25 mm of water deficit.

Mean annual water surplus and deficit values of 272.6 mm (± 96.6 mm) and 181.8 mm (± 46.7 mm), respectively, were observed in Alto Taquari microregion (Fig. 5). The localities of Alcinópolis (Fig. 5A) and Sonora (Fig. 6H) presented the highest values of water surplus in the microregion. The locality of Pedro Gomes (Fig. 5E) had the highest mean annual water deficit in Alto Taquari microregion

Aquidauana microregion presented a mean annual water surplus of 80.64mm (± 25.3 mm) and a mean annual water deficit of 141.4 mm (± 38.8 mm) (Fig. 6). Dois Irmãos do Buriti (Fig. 6C) presented the highest water surplus among the localities of the Aquidauana microregion. The municipality of Miranda (Fig. 6D) showed the highest water deficit in the microregion.

The mean annual water surplus in Baixo Pantanal microregion was 23.15 mm (± 23.6 mm), while its mean annual water deficit was 293.88 mm (± 144.2 mm), distributed from February to December (Fig. 6). This microregion undergoes more than nine months of water deficit. Among the localities of this microregion, Porto Murtinho (Fig. 6F) presented the highest water surplus, while Corumbá (Fig. 6E) and Ladário (Fig. 6G) had the same variation in water surplus and deficit.

Bodoquena microregion presented a mean annual water deficit of 72.56 mm (± 20.87), distributed from July to November, standing out September, which represents 37% of the water deficit (Fig. 7). The locality of Bodoquena (Fig. 7B) had the highest water deficit in the microregion, with a value of 120 mm year^{-1}. Bela Vista (Fig. 7A), Guia Lopes da Laguna (Fig. 7E), and Nioaque (Fig. 7G) presented the lowest water deficit values and stood out with the highest water surplus in the microregion.

Campo Grande microregion had a mean annual water surplus of 304.2 mm (± 28.3 mm) and a mean annual water deficit of 102.5 mm (± 30.4 mm), with the highest concentration from July to October (Fig. 8). The localities of Campo Grande (Fig. 9B) and Terenos (Fig. 8G) showed similar values of water surplus and deficit, as also observed for Corguinho (Fig. 8C) and Rochedo (Fig. 8F). Jaraguari (Fig. 8D) had the highest water surplus in Campo Grande microregion, while Rio Negro (Fig. 8E) had the highest mean annual water deficit.

Dourados microregion had a relatively low water deficit compared to other microregions, with a mean annual value of 17.1 mm (± 11.1 mm) concentrated from August to October (Fig. 9). The mean annual water surplus of the Dourados microregion was 287.48 mm (± 105 mm). The locality of Amambaí (Fig. 9A) presented the highest water surplus among localities of this microregion, besides a low water deficit of 3.87 mm. The water surplus index in the region was found in Vicentina (Fig. 9O), with a difference between both localities of 280 mm, showing a high variation in water surplus between localities of this microregion. Nova Alvorada do Sul (Fig. 9L) showed the highest and best-distributed water deficit, with a value of 46.98 mm, differing considerably in relation to other localities.

Iguatemi microregion has 16 municipalities and is the largest in territorial extension, among other microregions (Fig. 10). The locality of Sete Quedas (Fig. 10O) had the highest water surplus among localities. This microregion stood out for having high values of water surplus, showing an annual mean of 280.33 mm (± 122.4 mm). Deodápolis (Fig. 10C) had the highest water deficit, while Iguatemi showed the lowest values (Fig. 10F); this region had a mean water deficit of 9.32 mm (± 7.45 mm).

Nova Andradina microregion showed a water deficit value of 25.47 mm year^{-1} (± 17 mm). The municipality of Bataguassu (Fig. 11B) had the highest water deficit among the regional localities, representing 48% of the sum of the values. This microregion has a mean annual water surplus of 196.8 mm (± 102.84 mm). Among the regional localities, Anaurilândia (Fig. 11A) stood out because its mean annual value exceeded 300 mm, being well distributed from January to June and October to December.

Cassilândia microregion showed a mean annual water surplus of 419.17 mm (± 41.1 mm) and a mean annual water deficit of 145.3 mm (± 18.5 mm) (Fig. 11). The locality of Cassilândia (Fig. 11F) had the highest water deficit. Chapadão do Sul (Fig. 11H) presented the highest water surplus in this microregion. In addition, this

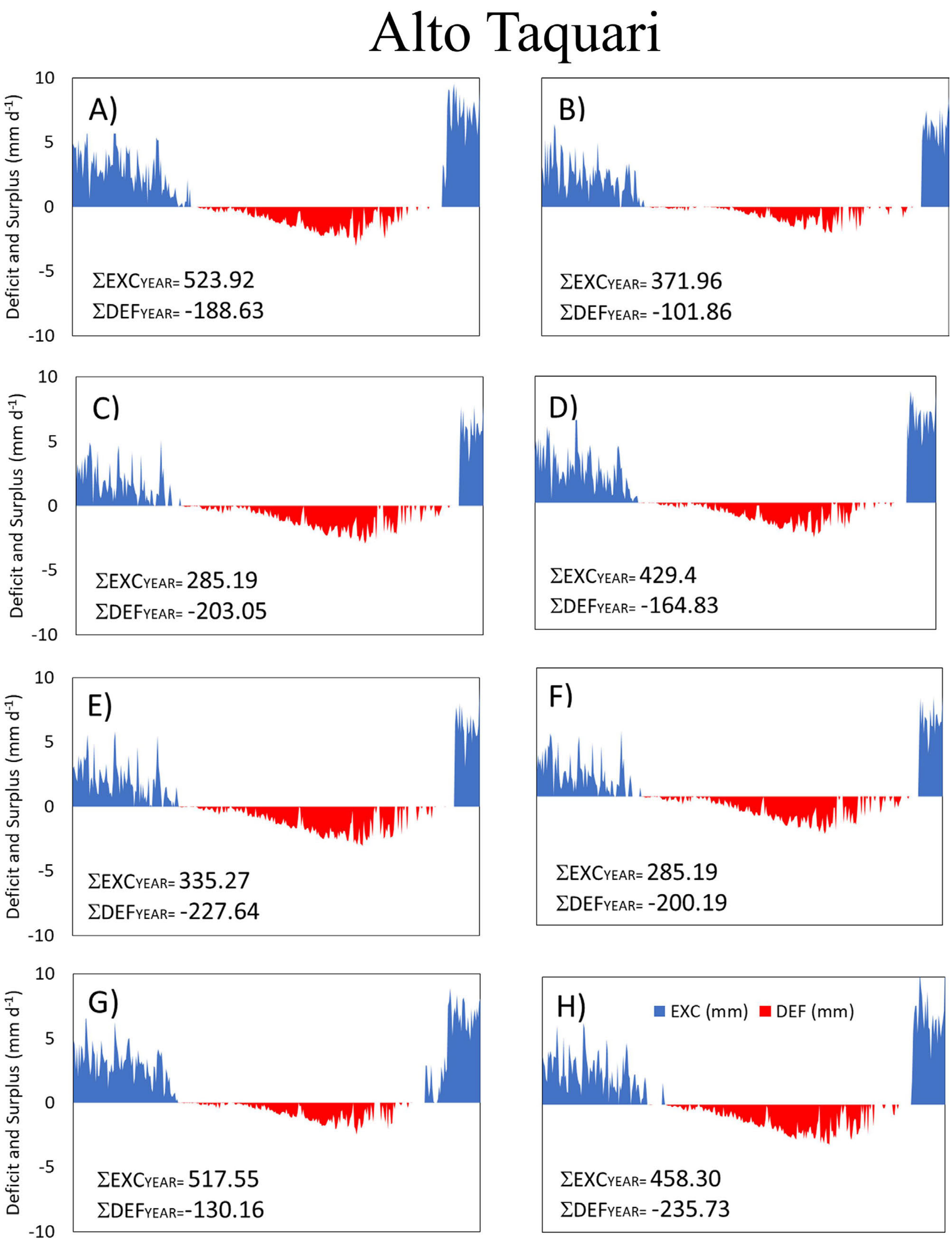

Figure 5 - Variation in water deficit and surplus for Alto Taquari microregion. A) Alcinópolis, B) Camapuã, C) Coxim, D) Figueirão, E) Pedro Gomes, F) Rio Verde do Mato Grosso, G) São Gabriel do Oeste, and H) Sonora.

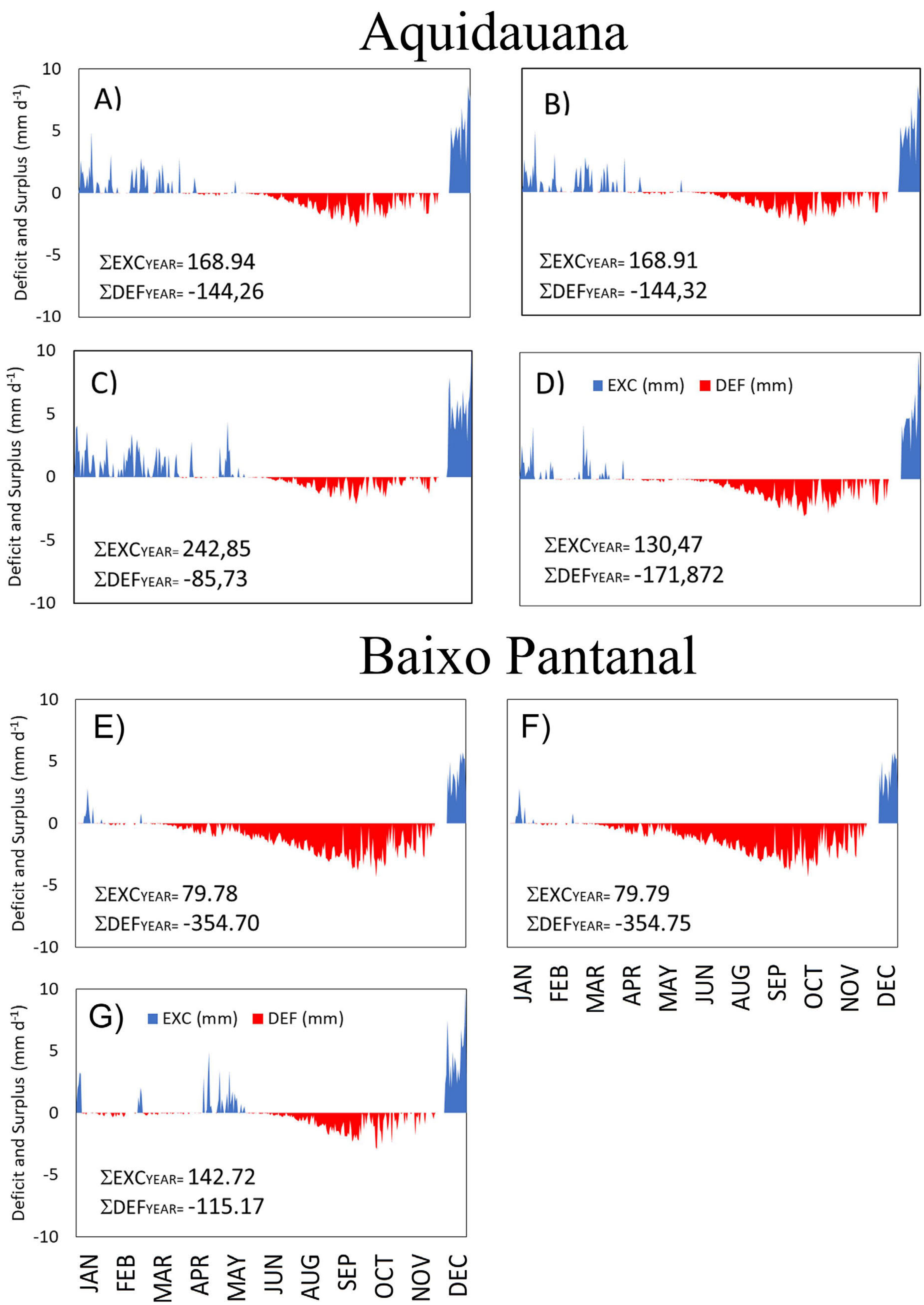

Figure 6 - Variation in water deficit and surplus for Aquidauana microregion. A) Anastácio, B) Aquidauana, C) Dois Irmãos do Buriti, D) Miranda and for Baixo Pantanal microregion. E) Corumbá, F) Ladário and G) Porto Murtinho.

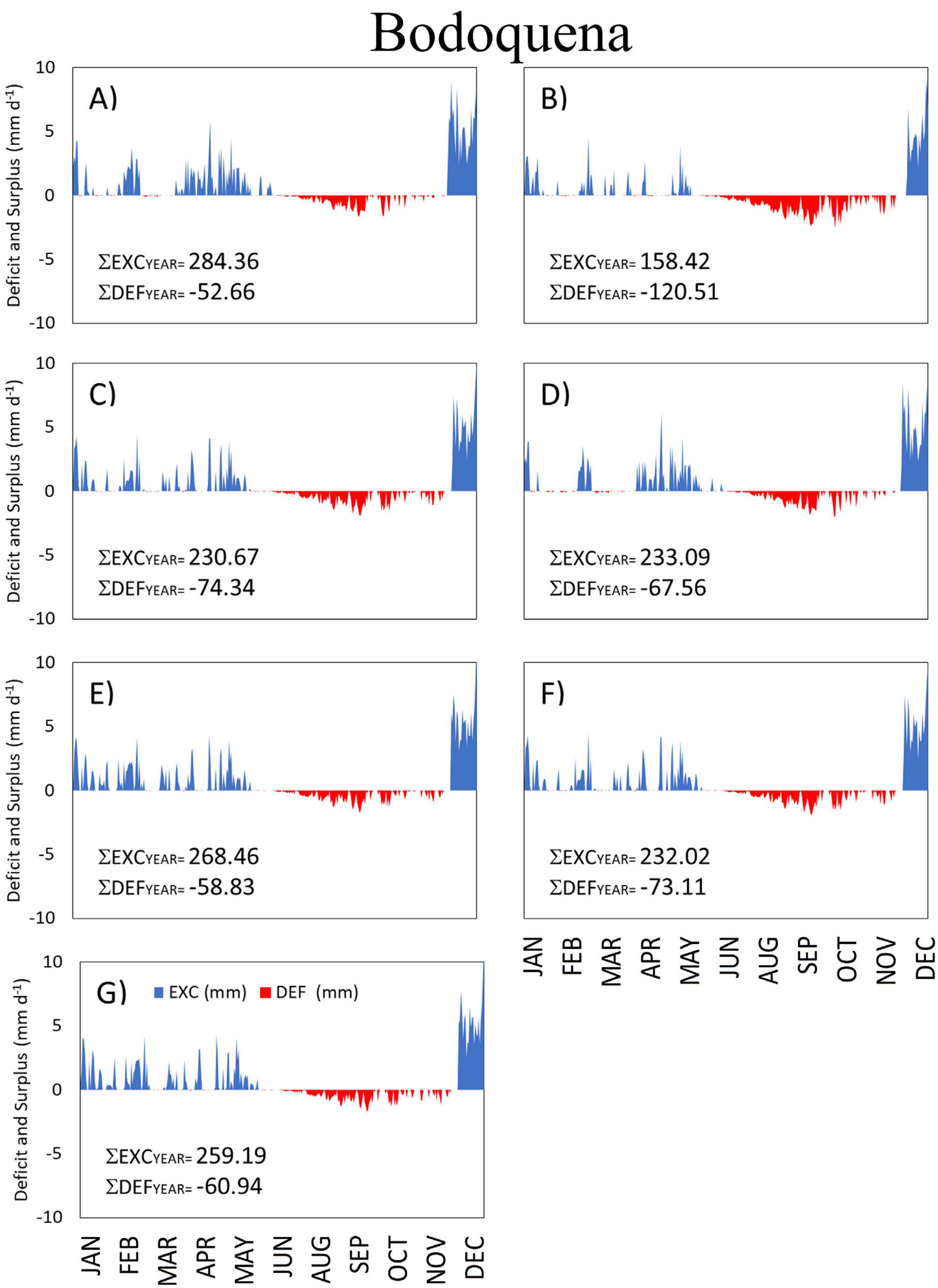

Figure 7 - Variation in water deficit and water surplus for Bodoquena microregion. A) Bela Vista, B) Bodoquena, C) Bonito, D) Caracol, E) Guia Lopes da Laguna, F) Jardim, and G) Nioaque.

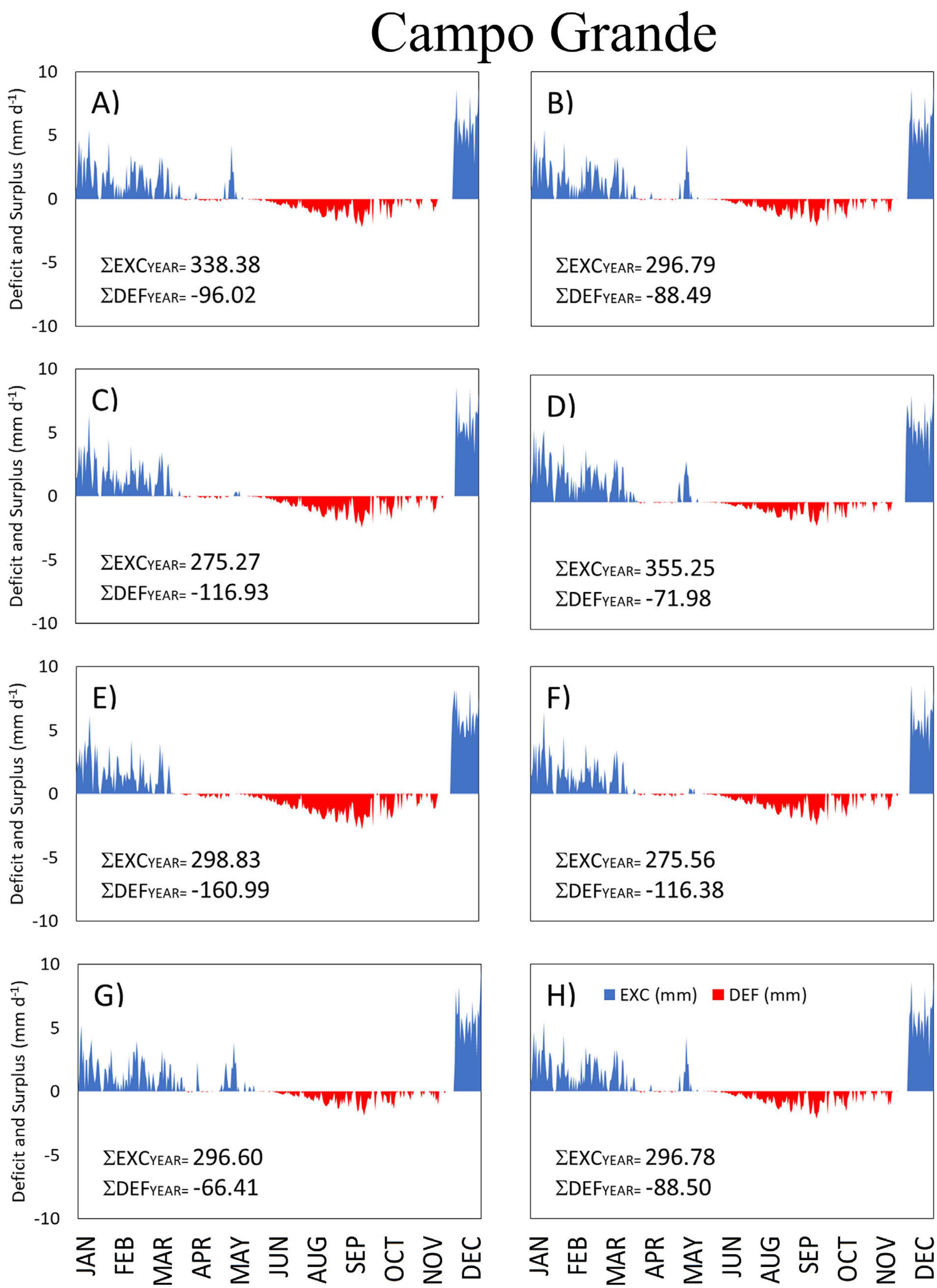

Figure 8 - Variation in water deficit and surplus for Campo Grande microregion. A) Bandeirantes, B) Campo Grande, C) Corguinho D) Jaraguari, E) Rio Negro, F) Rochedo, G) Sidrolândia, and H) Terenos.

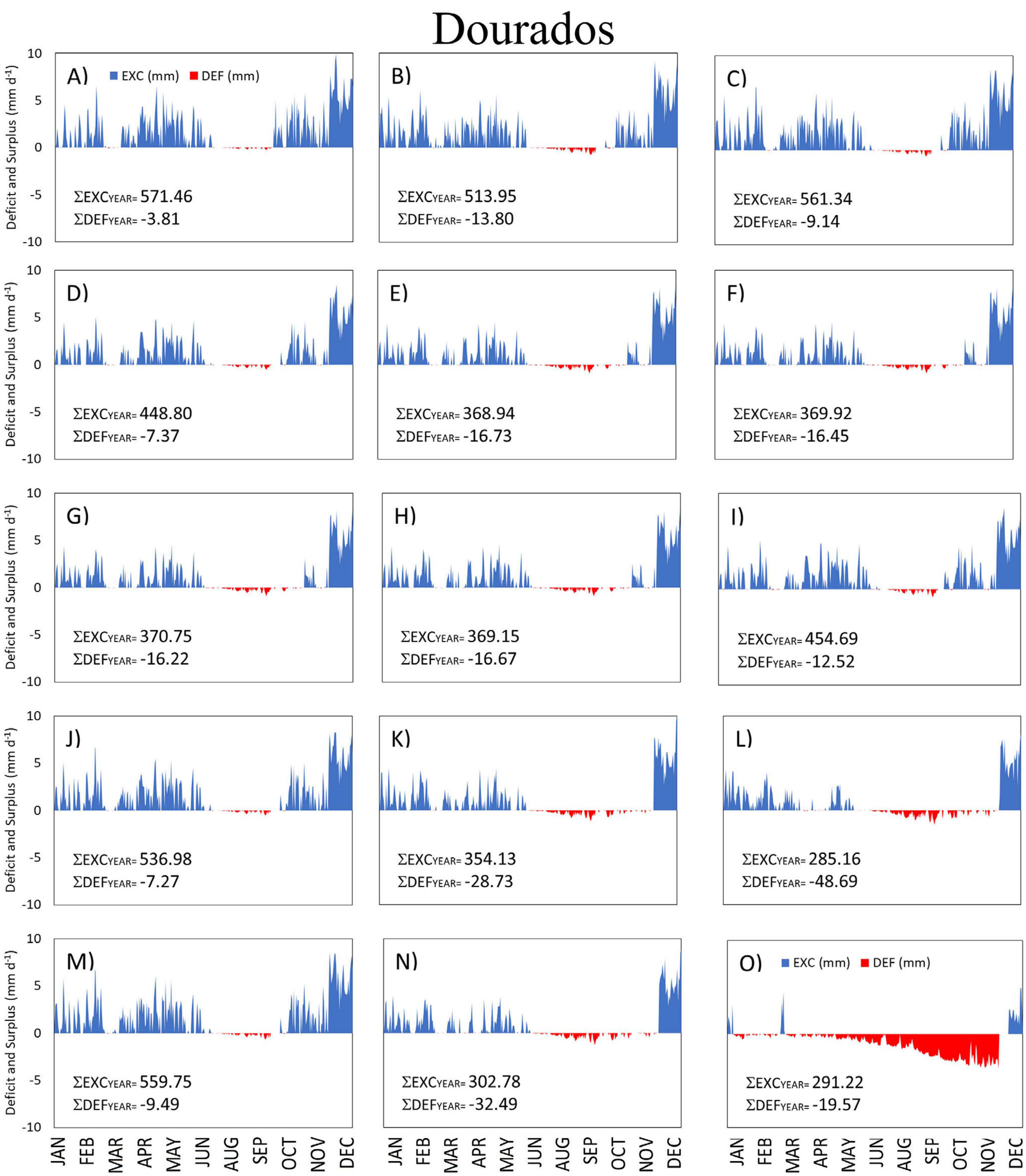

Figure 9 - Variation in water deficit and surplus for Dourados microregion. A) Amambaí, B) Antônio João, C) Aral Moreira D) Caarapó E) Douradina, F) Dourados, G) Fátima do Sul, H) Itaporã, I) Juti, J) Laguna Carapã, K) Maracaju, L) Nova Alvorada do Sul, M) Ponta Porã, N) Rio Brilhante, and O) Vicentina.

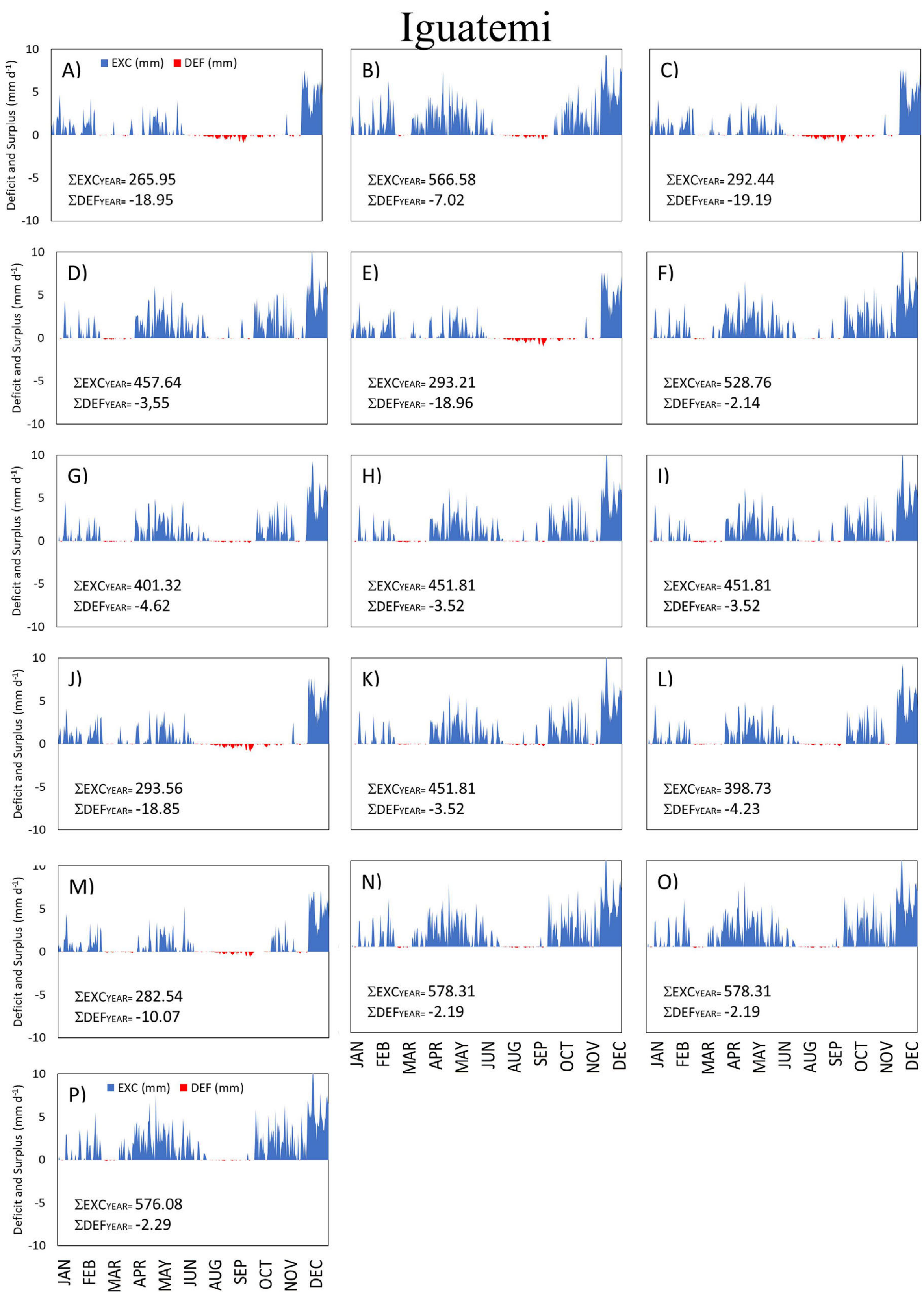

Figure 10 - Variation in water deficit and surplus for Iguatemi microregion. A) Angélica, B) Coronel Sapucaia, C) Deodápolis, D) Eldorado, E) Glória de Dourados, F) Iguatemi, G) Itaquiraí, H) Ivinhema, I) Japorã, J) Jateí, K) Mundo Novo, L) Naviraí, M) Novo Horizonte do Sul, N) Paranhos, O) Sete Quedas, and P) Tacuru.

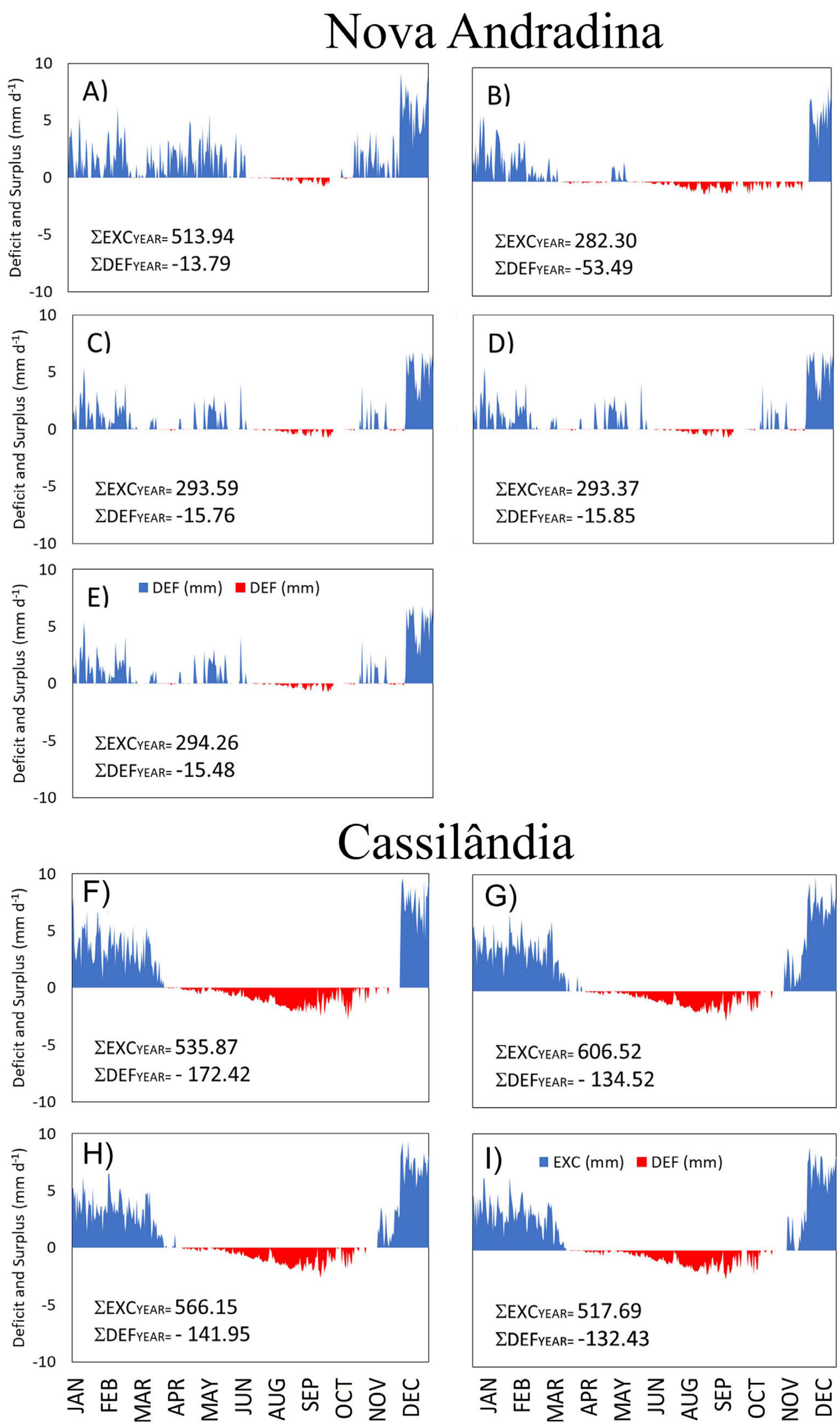

Figure 11 - Variation in water deficit and surplus for Nova Andradina microregion. A) Anaurilândia, B) Bataguassu, C) Bataiporã, D) Nova Andradina, E) Taquarussu and for Cassilândia microregion. F) Cassilândia, G) Chapadão do Sul, H) Costa Rica, and I) Paraíso das Águas.

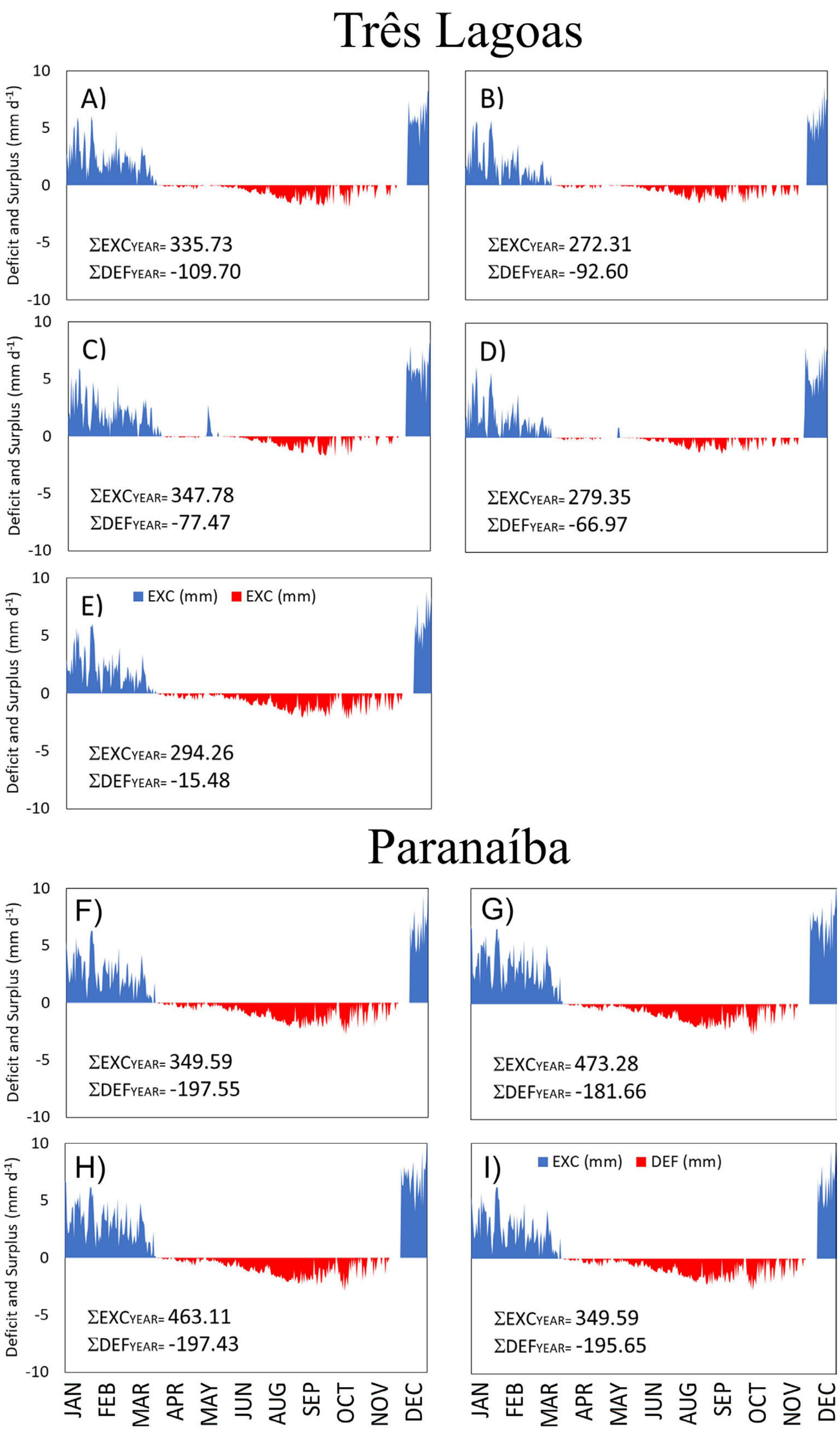

Figure 12 - Variation in water deficit and surplus for Três Lagoas microregion. A) Águas Claras, B) Brasilândia, C) Ribas do Rio Pardo, D) Santa Rita do Rio Pardo, E) Três Lagoas and for Paranaíba microregion. F) Aparecida do Taboado, G) Inocência, H) Paranaíba and I) Selvíria

microregion has a high water deficit and surplus simultaneously.

The mean annual water deficit in Três Lagoas microregion was 102.6 mm (± 39.1 mm), with a water surplus of 208 mm. The highest and lowest mean annual water surplus values were observed in Ribas do Rio Pardo (Fig. 12C) and Brasilândia (Fig. 12B), respectively. Moreover, the highest and lowest water deficit values were found in Águas Claras (Fig. 12A) and Santa Rita do Rio Pardo (Fig. 12C), respectively.

Paranaíba microregion had a mean annual water surplus of 408.89 mm (± 68.6 mm), as shown in Fig. 12. The municipality of Inocência (Fig. 12C) stood out for having 65 mm above the regional mean. Aparecida do Taboado (Fig. 12F) and Selvíria (Fig. 12I) presented the same water surplus. However, Aparecida do Taboado presented the highest water deficit in this microregion.

Mato Grosso do Sul had a high spatial variation in water deficit and surplus (Fig. 13AB). The increase in water surplus occurred from west to east of MS, with the highest values of water surplus concentrated in the south and north of the state. Baixo Pantanal microregion, located in the west, had the lowest water surplus values, while the regions of Cassilândia (north) and Iguatemi (south) showed the highest values.

Precipitation directly influences the soil water balance. (Marcuzzo *et al*., 2012) analyzed the spatial and seasonal variations of precipitation in the Cerrado biome of Mato Grosso do Sul. As a result, they highlight the north and southwest regions of the state, which concentrated the highest frequency of precipitation due to the influence of the continental equatorial air mass (from the north) and the Atlantic tropical air mass (from the east), mainly in the entire southern region. In addition, there is the orographic precipitation that occurs in the Serra da Bodoquena region.

The increase in water deficit in the microregions of MS occurred in the south-northwest direction (Fig. 13B), as shown in the strong negative correlation between latitude and water deficit. The highest water deficit values were observed as latitude decreased. Iguatemi microregion (south) showed the lowest water deficit, while Baixo do Pantanal (west) had the highest water deficit values.

According to the humidity index (Ih), the state of Mato Grosso do Sul presented four climate types, i.e., B1 (humid), B2 (humid), B3 (humid) and C2 (subhumid) (Fig. 13C), which was already expected due to the sensitivity of the Thornthwaite classification criteria (Rolim *et al*., 2007). The B1 index was more prevalent in the state, covering 59.27% of all localities, while B3 had the lowest presence, covering only 0.63% of the state. Baixo Pantanal microregion, located in the west of MS, presented the highest water deficit value, being classified as subhumid. Microregions with the highest water surplus values, such

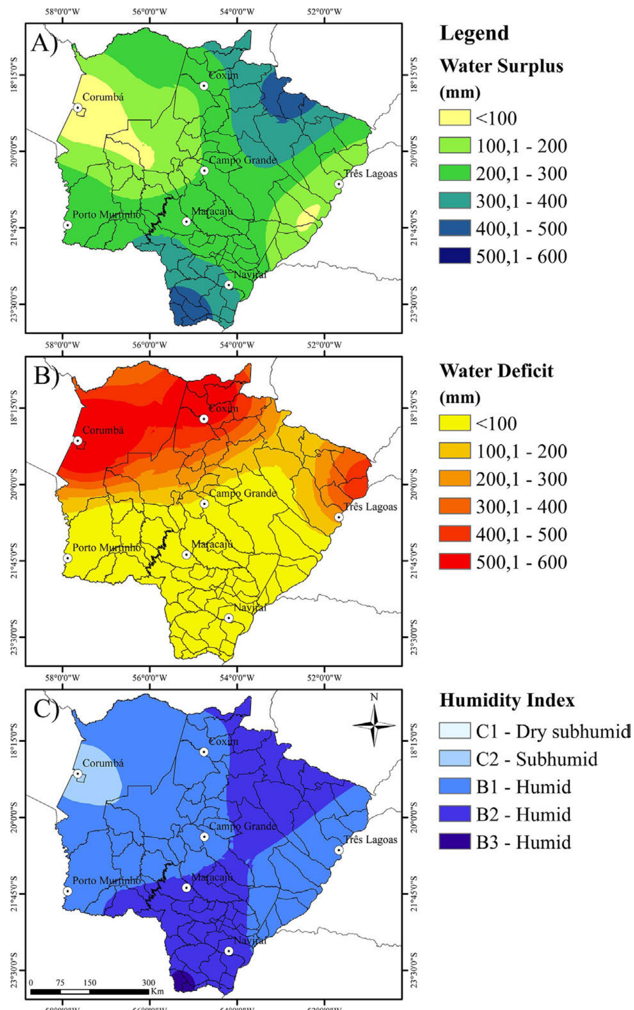

Figure 13 - Spatial distribution of water surplus (A), water deficit (B) and humidity index (C) in Mato Grosso do Sul, Brazil.

as Cassilândia and Iguatemi, were classified as B2 (humid).

The municipality of Chapadão do Sul, located in Cassilândia microregion, was classified as having the climate type B3. This municipality had mean annual water surplus and deficit values of 606.52 and 134.54 mm, respectively. These indices can be useful in mesoscale or toposcale studies, in which the effects of topography directly interfere with climatic elements and, consequently, planning of regional agricultural, environmental, and forestry activities (Araújo *et al*., 2016; Rolim *et al*., 2007).

The knowledge of the regional climate results in sustainable and more profitable systems, in addition to greater food security (Henry and Krutz, 2016). The introduction of smart farming practices, such as the use of weather stations, is interesting to deal with changes in agroclimatic zones, which lead to changes in cultivation patterns.

In relation to the possible scenarios of climatic worldliness, between the period 2041-2060, there was a great variation in the distribution of the humid index in the state of Mato Grosso do Sul (Fig. 14). The main changes of the current scenario (Fig. 14 C), with climatic scenarios, were the spressive reduction of the wettest climatic classes (B3, B2 and B1), and the presence of another climatic class, C1 - Dry subhumid, being the driest class among all in the state.

In RCP 2.6, there was a small increase in class B3, of 1% and in class C1 of 58% compared to the current scenario (Fig. 14A). There was also a large reduction in classes B2 and B1, of 30 and 33%, respectively, thus reducing the state wet (Table 1). In RCP 4.5, class C1 had great representativeness, with 42% of all territory, being the driest among all scenarios in the period 2041-2060 (Fig. 14B). The RCP 4.5 scenario demonstrates higher concentration of greenhouse gases over the medium term

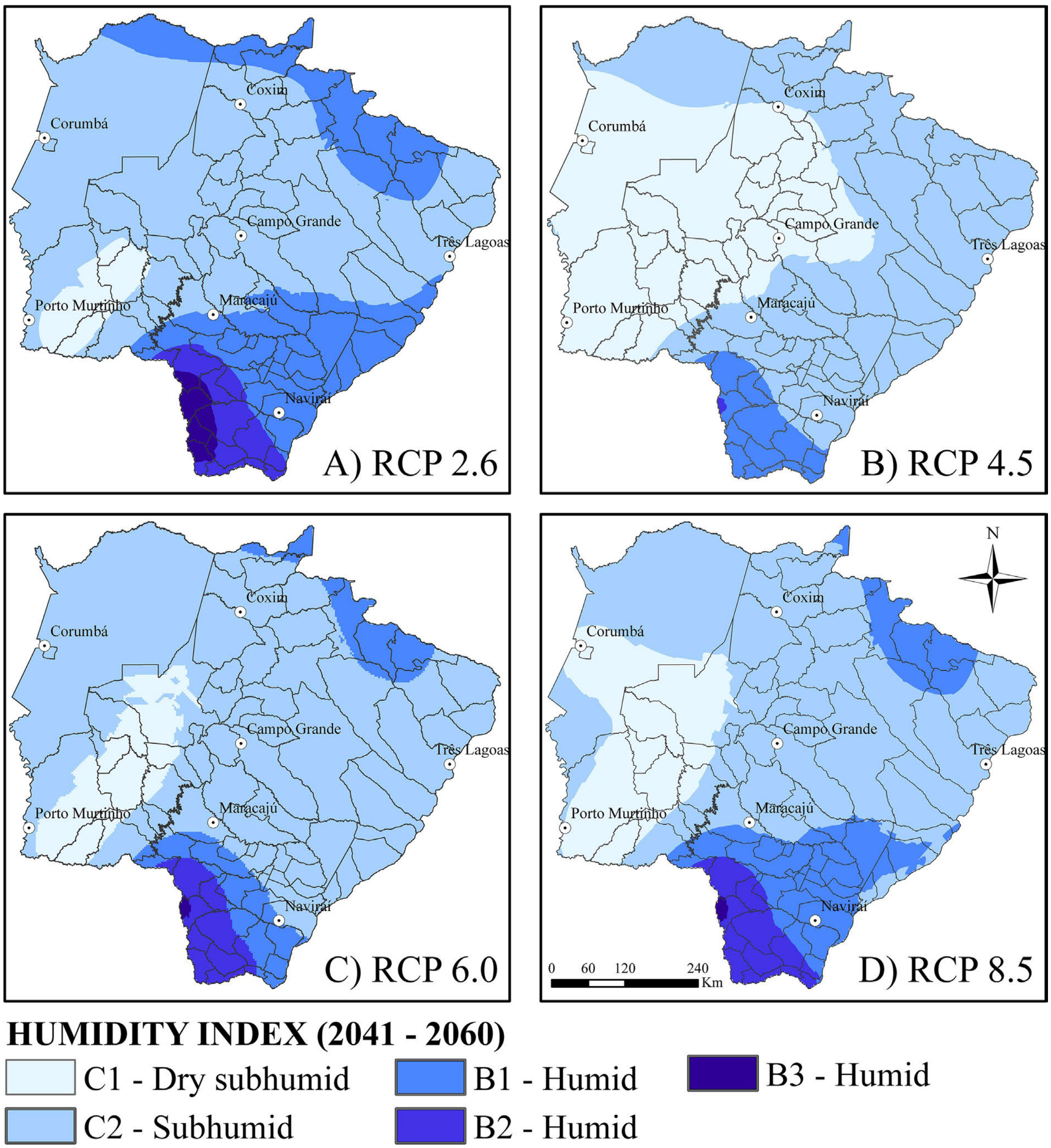

Figure 14 - Spatial distribution of humidity index in 2041 - 2060. Legend: A) RCP 2.6, B) RCP 4.5, C) RCP 6.0 and D) RCP 8.5

(2041-2060), thus being warmer in relation to the others (Chou *et al*., 2014). Evidencing a great concern, since this great reduction in the humidity of the state can lead to a decrease in agricultural productivity in the region (Junqueira *et al*., 2017; Srivastava *et al*., 2018). RCPs 6.0 and 8.5 were very similar, with a large predominance of class C2 - Subhumid, with 65% of the total area approximately (Fig. 14 C D).

The climatic projections for 2061 - 2080 showed great impacts on the water dynamics of the state, with greater prominence in the northwest region of the state (Fig. 15). All scenarios showed a reduction in the area classified as wet (B1, B2 and B3), in relation to the current climatological normal (1960 - 1990). The RCP scenario 8.5 stood out as the driest, being only 6.80% of the state area classified as wet (Fig. 15 D, Table 1). On the other

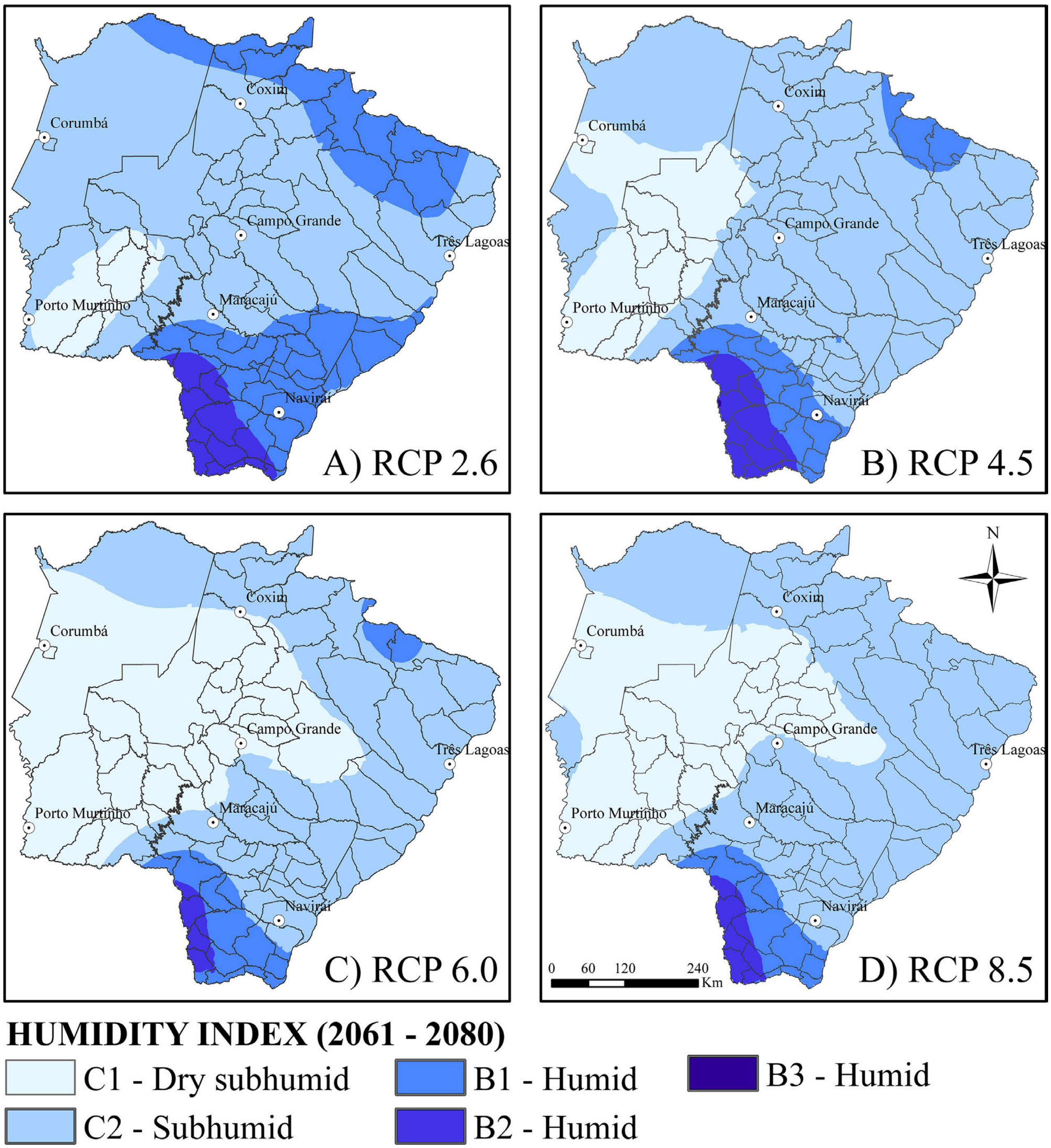

Figure 15 - Spatial distribution of humidity index in 2061 - 2080. Legend: A) RCP 2.6, B) RCP 4.5, C) RCP 6.0 and D) RCP 8.

Table 1 - Percentage of the territory of Mato Grosso do Sul for the classes of humidity index, in the current scenario and in the RCP's for the periods of 2041 - 2060 and 2061 - 2080.

	C1 Dry subhumid	C2 Subhumid	B1 Humid	B2 Humid	B3 Humid
		1960-1990			
Current (%)	-	4.28	59.27	35.82	0.63
		2041-2060			
RCP 2.6 (%)	4.63	62.65	26.50	4.54	1.68
RCP 4.5 (%)	42.24	52.07	5.63	0.07	-
RCP 6.0 (%)	9.49	76.64	9.65	4.09	0.13
RCP 8.5 (%)	17.93	60.56	16.41	4.94	0.16
		2061-2080			
RCP 2.6 (%)	6.26	62.38	26.66	4.69	-
RCP 4.5 (%)	18.92	68.14	8.72	4.20	0.02
RCP 6.0 (%)	44.15	48.09	6.41	1.35	-
RCP 8.5 (%)	35.37	57.65	4.89	2.09	-

hand, the RCP scenario 4.5 showed a higher concentration of wet classes in relation to the period 2041 - 2060, a state that increased the concentration of greenhouse gases between this period (Van Vuuren *et al*., 2011).

The impact of climatic mundanças on the humidity index of the state was not homogeneous, some regions underwent greater changes in the other alterations (Fig. 15). The western and northwest regions of the state showed a reduction in humidity in all scenarios, with greater emphasis on RCP 6.0 and 8.5, in which practically both regions were classified as subhumid dry (C1). These changes can have a great impact for the west and northwest regions, considering that it concentrates 65% of the Pantanal biome, impairing its water dynamics, thus harming the fauna and flora of the biome (Marengo *et al*., 2015).

4. Conclusion

The prevailing climate in the state of Mato Grosso do Sul is classified as C2 (moist subhumid). Mato Grosso do Sul has two well-defined periods over the year: a dry and a rainy period. The three climate types that predominate in MS, according to the Thornthwaite (1948) classification, are B1 (humid), B2 (humid), B3 (humid) and C2 (moist subhumid).

The water characterization of Mato Grosso do Sul showed 234.78 mm year^{-1} of water surplus, 80.8 mm year^{-1} of water deficit, and 1,114.8 mm year^{-1} of potential evapotranspiration. Water deficit and potential evapotranspiration decrease as latitude increases.

The climatic projections show, in all scenarios, reduce the area classified as umida in the state (B1, B2 and B3), besides adding the dry subhumid class (C1). The Scenario RCP 8.5 in 2061-2080 is the most worrisome situation of all, because the state can undergo major changes, especially in the Pantanal biome region.

Acknowledgment

This work was done with financial support from Instituto Federal de Mato Grosso do Sul - IFMS.

References

ABRECHT, D.G.; CARBERRY, P.S. The influence of water deficit prior to tassel initiation on maize growth, development and yield. **Field Crops Research**, v. 31, n. 1, p. 55-69, 1993.

ADEFISAN, E. Climate change impact on rainfall and temperature distributions over West Africa from three IPCC scenarios. **Journal of Earth Science & Climatic Change**, v. 9, n. 6, 1000476, 2018. doi

AKAS, P.S.; HIDAYANTO, M.; FIANA, Y. Analysis of water balance to determine cropping patterns of food crop in subwatershed Tenggarong, Kutai Kartanegara regency. **Bulgarian Journal of Agricultural Science**, v. 25, n. 1, p. 215-221, 2019.

APARECIDO, L.E.O.; MENESES, K.C.; TORSONI, G.B.; MORAES, J.R.S.C.; MESQUITA, D.Z. Accuracy of potential evapotranspiration models in different time scales. **Revista Brasileira de Meteorologia**, v. 35, n. 1, p. 63-80, 2020.

APARECIDO, L.E.O.; ROLIM, G.S.; RICHETTI, J.; SOUZA, P.S.; JOHANN, J.A. Köppen, Thornthwaite and Camargo climate classifications for climatic zoning in the State of Paraná, Brazil. **Ciência e Agrotecnologia**, v. 40, n. 4, p. 405-417, 2016.

ARAÚJO, R.; ALVES JUNIOR, J.; CASAROLI, D.; EVANGELISTA, A.W.P. Variação na qualidade da matéria-prima da cana-de-açúcar em decorrência da suspensão da irrigação antes da colheita e da ocorrência de baixas temperaturas. **Bragantia**, v. 75, n. 1, p. 118-127, 2016.

BOER, G.J.; FLATO, G.; RAMSDEN, D. A transient climate change simulation with greenhouse gas and aerosol forcing: experimental design and comparison with the instrumental record for the twentieth century. **Climate Dynamics**, v. 16, n. 6, p. 405-425, 2000.

BRUNEL-SALDIAS, N.; SEGUEL, O.; OVALLE, C.; ACEVEDO, E.; MARTÍNEZ, I. Tillage effects on the soil water balance and the use of water by oats and wheat in a Mediterranean climate. **Soil and Tillage Research**, v. 184, p. 68-77, 2018.

CASONATO, L. The role of agribusiness in Mato Grosso do Sul's economic growth in the light of Solow's model, Brazil. **Revista de Economia Agrícola**, v. 60, n. 1, p. 31-39, 2013.

CECÍLIO, R.A.; SILVA, K.R.; XAVIER, A.C.; PEZZOPANE, J.R.M. Método para a espacialização dos elementos do balanço hídrico climatológico. **Pesquisa Agropecuária Brasileira**, v. 47, n. 4, p. 478-488, 2012.

CEGLAR, A.; TORETI, A.; LECERF, R.; VELDE, M.V.D.; DENTENER, F. Impact of meteorological drivers on regional inter-annual crop yield variability in France. **Agricultural and Forest Meteorology**, v. 216, p. 58-67, 2016.

CHOU, S.C.; LYRA, A.; MOURÃO, C.; DERECZYNSKI, C.; PILOTTO, I.; GOMES, J. *et al*. Assessment of climate change over South America under RCP 4.5 and 8.5 downscaling scenarios. **American Journal of Climate Change**, v. 3, n. 5, p. 512-527, 2014.

CLARKE, R.T. The relation between interannual storage and frequency of droughts, with particular reference to the Pantanal Wetland of South America. **Geophysical Research Letters**, v. 32, n. 5, p. L05402, 2005.

CLARKE, R.T. The relation between interannual storage and frequency of droughts, with particular reference to the Pantanal Wetland of South America. **Geophysical Research Letters**, v. 32, n. 5, p. L05402, 2005.

CUNHA, F.F.; MAGALHÃES, F.F.; CASTRO, M.A.D.; SOUZA, E.J.D. Performance of estimative models for daily reference evapotranspiration in the city of Cassilândia, Brazil. **Engenharia Agrícola**, v. 37, n. 1, p. 173-184, 2017.

DANTAS, A.A.A.; CARVALHO, L.G.; FERREIRA, E. Climatic classification and tendencies in Lavras region, MG. **Ciência e Agrotecnologia**, v. 31, p. 1862-1866, 2007.

DE SÁ JÚNIOR, A.; DE CARVALHO, L.G.; DA SILVA, F.F.; DE CARVALHO ALVES, M. Application of the Köppen classification for climatic zoning in the state of Minas Gerais, Brazil. **Theoretical and Applied Climatology**, v. 108, n. 1, p. 1-7, 2012.

ELGUINDI, N.; GRUNDSTEIN, A.; BERNARDES, S.; TURUNCOGLU, U.; FEDDEMA, J. Assessment of CMIP5 global model simulations and climate change projections for the 21 st century using a modified Thornthwaite climate classification. **Climatic change**, v. 122, n. 4, p. 523-538, 2014.

FEDDEMA, J.J. A revised Thornthwaite-type global climate classification. **Physical Geography**, v. 26, n. 6, p. 442-466, 2005.

FLATO, G.; MAROTZKE, J.; ABIODUN, B.; BRACONNOT, P.; CHOU, S.C. Evaluation of climate models. In: **Climate Change 2013: The Physical Science Basis. Contribution of Working Group I to the Fifth Assessment Report of the Intergovernmental Panel on Climate Change**. Cambridge: Cambridge University Press, v. 7, p. 741-866, 2014.

GENG, J.; MATSUDA, K.; FU, L.; FAGNARD, J.-F.; ZHANG, H.; ZHANG, X. Origin of dc voltage in type II superconducting flux pumps: field, field rate of change, and current density dependence of resistivity. **Journal of Physics D: Applied Physics**, v. 49, n. 11, p. 11LT01, 2016.

HARTIN, C.A.; PATEL, P.; SCHWARBER, A.; LINK, R.P.; BOND-LAMBERTY, B.P. A simple object-oriented and open-source model for scientific and policy analyses of the global climate system-Hector v1. 0. **Geoscientific Model Development**, v. 8, n. 4, p. 939-955, 2015.

HENRY, W.B.; KRUTZ, L.J. Water in agriculture: Improving corn production practices to minimize climate risk and optimize profitability. **Current Climate Change Reports**, v. 2, n. 2, p. 49-54, 2016.

HOLM, P.; WINIWARTER, V. Climate change studies and the human sciences. **Global and Planetary Change**, v. 156, p. 115-122, 2017.

HOSSAIN, M.A.; PAUL, S.C.; MANDAL, A.C. Natural convection flow along a vertical circular cone with uniform surface temperature and surface heat flux in a thermally stratified medium. **International Journal of Numerical Methods for Heat & Fluid Flow**, v. 12, n. 3, p. 290-305, 2002.

JUNQUEIRA, T.L.; CHAGAS, M.F.; GOUVEIA, V.L.; REZENDE, M.C.; WATANABE, M.D. *et al.* Techno-economic analysis and climate change impacts of sugarcane biorefineries considering different time horizons. **Biotechnology for biofuels**, v. 10, n. 1, p. 1-12, 2017.

MARCUZZO, F.F.N.; MELO, D.C.R.; COSTA, H.C. Sazonalidade e distribuição espaço-temporal das chuvas no bioma do Cerrado do estado do Mato Grosso do Sul. **Revista Brasileira de Recursos Hídricos**, v. 17, p. 77, 2012.

MHLANGA, B.; THIERFELDER, C. Long-term conservation agriculture improves water properties and crop productivity in a Lixisol. **Geoderma**, v. 398, p. 115107, 2021.

MICHALAK, D. Adapting to climate change and effective water management in Polish agriculture-At the level of government institutions and farms. **Ecohydrology & Hydrobiology**, v. 20, n. 1, p. 134-141, 2020.

MOHAMMAD, A.; SUDHISHRI, S.; DAS, T.K.; SINGH, M.; BHATTACHARYYA, R. *et al.* Water balance in direct-seeded rice under conservation agriculture in North-western Indo-Gangetic Plains of India. **Irrigation Science**, v. 36, n. 6, p. 381-393, 2018.

MONTOYA, F.; GARCÍA, C.; PINTOS, F.; OTERO, A. Effects of irrigation regime on the growth and yield of irrigated soybean in temperate humid climatic conditions. **Agricultural Water Management**, v. 193, p. 30-45, 2017.

OMETTO, J. C. **Bioclimatologia Vegetal**. São Paulo: Agronômica Ceres, 1981.

PAGLIAI, M.; VIGNOZZI, N.; PELLEGRINI, S. Soil structure and the effect of management practices. **Soil and Tillage Research**, v. 79, n. 2, p. 131-143, 2004.

PASSOS, M.L.V.; ZAMBRZYCKI, G.C.; PEREIRA, R.S. Water balance and climatic classification for a given region of Chapadinha-MA. **Revista Brasileira de Agricultura Irrigada**, v. 10, n. 4, p. 758-766, 2016.

PEREIRA, A.R.; PAES DE CAMARGO, Â. An analysis of the criticism of thornthwaite's equation for estimating potential evapotranspiration. **Agricultural and Forest Meteorology**, v. 46, n. 1-2, p. 149-157, 1989.

ROLIM, G.S.; CAMARGO, M.B.P.; LANIA, D.G.; MORAES, J.F.L. de Climatic classification of Köppen and Thornthwaite sistems and their applicability in the determination of agroclimatic zonning for the state of São Paulo, Brazil. **Bragantia**, v. 66, n. 4, p. 711-720, 2007.

SRIVASTAVA, A.K.; MBOH, C.M.; ZHAO, G.; GAISER, T.; EWERT, F. Climate change impact under alternate realizations of climate scenarios on maize yield and biomass in Ghana. **Agricultural Systems**, v. 159, p. 157-174, 2018.

THAYER, A.W.; VARGAS, A.; CASTELLANOS, A.A.; LAFON, C.W.; MCCARL, B.A.; ROELKE, D.L. Integrating agriculture and ecosystems to find suitable adaptations to climate change. **Climate**, v. 8, n. 1, p. 10, 2020.

THORNTHWAITE, C.W. An approach toward a rational classification of climate. **Geographical Review**, v. 38, n. 1, p. 55-94, 1948.

THORNTHWAITE, C.W.; MATHER, J.R. The water balance climatology. **Laboratory of Climatology**, v. 8, p. 104, 1955.

van VUUREN, D.P.; EDMONDS, J.; KAINUMA, M.; RIAHI, K.; THOMSON, A. The representative concentration pathways: an overview. **Climatic change**, v. 109, n. 1, p. 5-31, 2011.

ZORTÉA, M.; DE SOUZA GOMES, K.; TOMAZ, L.A.G.; PALMEIRIM, J.M.M.M.; LIMA-RIBEIRO, M.S. Impacts of a hydroelectric power plant on the bat community in central Brazil. **Mammal Research**, v. 66, n. 3, p. 509-518, 2021.